

Helical Order in Tarantula Thick Filaments Requires the “Closed” Conformation of the Myosin Head

M. E. Zoghbi^{1,2*}, J. L. Woodhead¹, R. Craig¹ and R. Padrón²

¹Department of Cell Biology
University of Massachusetts
Medical School, 55 Lake Avenue
North, Worcester, MA 01655
USA

²Departamento de Biología
Estructural, Instituto
Venezolano de Investigaciones
Científicas (IVIC), Apdo 21827
Caracas 1020A, Venezuela

Myosin heads are helically ordered on the thick filament surface in relaxed muscle. In mammalian and avian filaments this helical arrangement is dependent on temperature and it has been suggested that helical order is related to ATP hydrolysis by the heads. To test this hypothesis, we have used electron microscopy and image analysis to study the ability and temperature dependence of analogs of ATP and ADP.Pi to induce helical order in tarantula thick filaments. ATP or analogs were added to rigor myofibrils or purified thick filaments at 22 °C and 4 °C and the samples negatively stained. The ADP.Pi analogs ADP.AIF₄ and ADP.Vi, and the ATP analogs ADP.BeF_x, AMPPNP and ATPγNH₂, all induced helical order in tarantula thick filaments, independent of temperature. In the absence of nucleotide, or in the presence of ADP or the ATP analog, ATPγS, there was no helical ordering. According to crystallographic and tryptophan fluorescence studies, all of these analogs, except ATPγS and ADP, induce the “closed” conformation of the myosin head (in which the γ phosphate pocket is closed). We suggest that helical order requires the closed conformation of the myosin head but is not dependent on the hydrolysis of ATP.

© 2004 Elsevier Ltd. All rights reserved.

Keywords: striated muscle; myosin filaments; helical order; ATP analogs; temperature

*Corresponding author

Introduction

Muscle contraction occurs by the sliding of the thin filaments past the thick filaments. Force is generated by the cyclic interaction of myosin heads with actin. In resting conditions (ATP and low calcium) myosin heads are detached from actin filaments. X-ray diffraction of muscle^{1–5} and electron microscopy of isolated thick filaments^{6–13} shows that detached heads in the relaxed state are helically ordered (or approximately so) around the backbone of the thick filament. We are interested in understanding the molecular basis and physiological relevance of this helical organization.

Thick filaments from invertebrates share basic structural parameters with vertebrate thick filaments although they are larger in diameter and length. Because invertebrate filaments have a well-

ordered and stable helical arrangement they represent a very useful system for studying the relaxed organization of heads. Several three-dimensional reconstructions have been calculated for negatively stained thick filaments^{6,8–13} and the 3D map for tarantula thick filaments has resolved the individual myosin heads.⁸ The molecular basis of the helical ordering of the heads is not well understood, although in the case of tarantula muscle thick filaments, interactions between antiparallel heads from successive crowns appear to be involved.^{8,14}

Establishment of helical order appears to require the presence of ATP^{1,2,15–17} and it has been suggested that it is the specific chemical state of the ATP (i.e. pre- or post-hydrolysis) trapped in the active site of the myosin heads that determines whether helical ordering occurs.^{18–20} Rabbit thick filaments become disordered at temperatures below 20 °C, and this has been attributed to a lowering of the rate of ATP hydrolysis by myosin. It was suggested that helical order is established only after the hydrolytic step, when the ADP.Pi produced is bound at the active site.¹⁸ This suggestion was supported by X-ray diffraction patterns of rabbit skeletal muscle exposed to different nucleotides at different temperatures¹⁹ (although

Abbreviations used: AMPPNP, adenosine 5'-(β,γ-imido) triphosphate; ATPγNH₂, γ-amido adenosine 5'-triphosphate; ATPγS, adenosine 5'-[γ-thio] triphosphate; AP₅A, diadenosine pentaphosphate; FFT, fast Fourier transform; Pi, phosphate; Vi, vanadate.

E-mail address of the corresponding author:
maria.zoghbi@umassmed.edu

the possibility of a coupling between the helical order and a specific conformation of the myosin head that may depend on the bound nucleotide was also considered as an alternative). However, while warm-blooded animals (chicken as well as rabbit) require warm temperatures ($>20^{\circ}\text{C}$) for helical ordering,^{18–22} cold-blooded animals, such as frog and fish, do not,^{23–25} and the dependence of helical order on the chemical state of ATP in thick filaments from cold-blooded animals has not yet been studied.

Here, we have used a cold-blooded species to test the hypothesis that helical ordering of the heads requires ATP hydrolysis. We have studied the dependence of the helical order on both the temperature and the chemical state of the bound nucleotide in native thick filaments from tarantula. We observe a small dependence of helical order on temperature in the presence of the naturally occurring nucleotide (ATP), but no dependence on the chemical state of the ATP. Instead, helical ordering appears to require a specific conformation of the myosin head: the so called “closed” conformation that has been reported in crystallographic studies (see Geeves & Holmes²⁶ for a review). In this closed conformation switch 1 and switch 2 are near to the nucleotide, keeping the γ phosphate pocket closed (although the actin-binding cleft is open).^{26–28} This work has been presented in preliminary form.²⁹

Results

Myofibrils can be used to study the effect of nucleotides on the ordering of myosin heads

Permeabilization and homogenization of muscle in rigor conditions produced a suspension of myofibrils where thin and thick filaments were strongly bound through cross-bridges (Figure 1a). When 5 mM MgATP was added to myofibrils in suspension, thick and thin filaments dissociated from each other and the thick filaments appeared helically ordered (Figure 1b). In the same way, we determined if the analogs of ATP or ADP.Pi induced helical order when they were added to myofibrils in suspension.

ATP induced helical ordering of tarantula thick filaments at 22°C and 4°C

Thick filaments in the presence of ATP showed helical order at 22°C (Figure 2a) and 4°C (Figure 2b). Fourier transforms of well-stained regions of filaments were computed to analyze the ordering. The transforms revealed layer-lines indexing on a repeat of ~ 43 nm, confirming the visual appearance of helical order (insets). Layer-lines were evident at both temperatures, indicating that helical order in tarantula thick filaments is maintained even at low temperature.

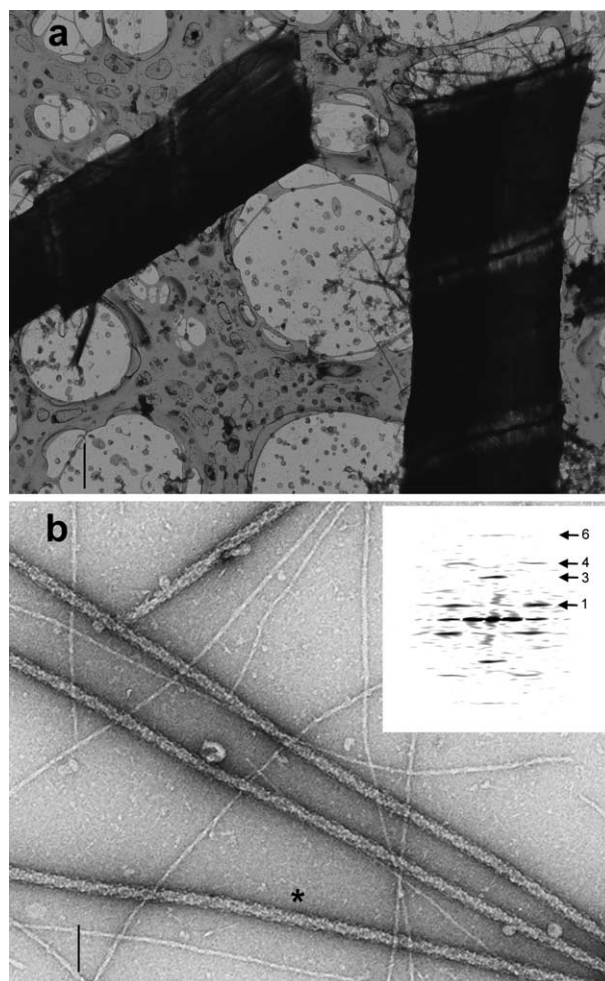


Figure 1. a, Washed myofibrils from muscle homogenate in rigor conditions. b, Addition of 5 mM MgATP caused dissociation of the thick from the thin filaments. The thick filaments were helically ordered (evident by viewing along the filament at a glancing angle). The inset in b is the Fourier transform of the filament indicated by the asterisk. Transforms in this and other Figures are oriented with the filament axis vertical, regardless of the filament orientation shown in the micrographs. The transform shows strong layer-lines based on a ~ 43 nm helical repeat (layer-lines 1 and 4, and the meridionals 3 and 6 are numbered). The specimens in all electron micrographs were negatively stained with 1% uranyl acetate. Scale bars represent 1 μm in a and 100 nm in b.

ATP γ S induced dissociation but not helical order, while AMPPNP and ATP γ NH $_2$ did not induce dissociation of myofibrils

Three ATP analogs (ATP γ S, AMPPNP and ATP γ NH $_2$) gave two different results (Figure 3). ATP γ S dissociated thin and thick filaments from each other, but failed to induce helical order in the thick filaments at either 22°C (Figure 3a) or 4°C (not shown). With AMPPNP and ATP γ NH $_2$ no separation of the filaments occurred (Figure 3b and c). Because thick and thin filaments did not dissociate (even up to 30 mM nucleotide), it was not

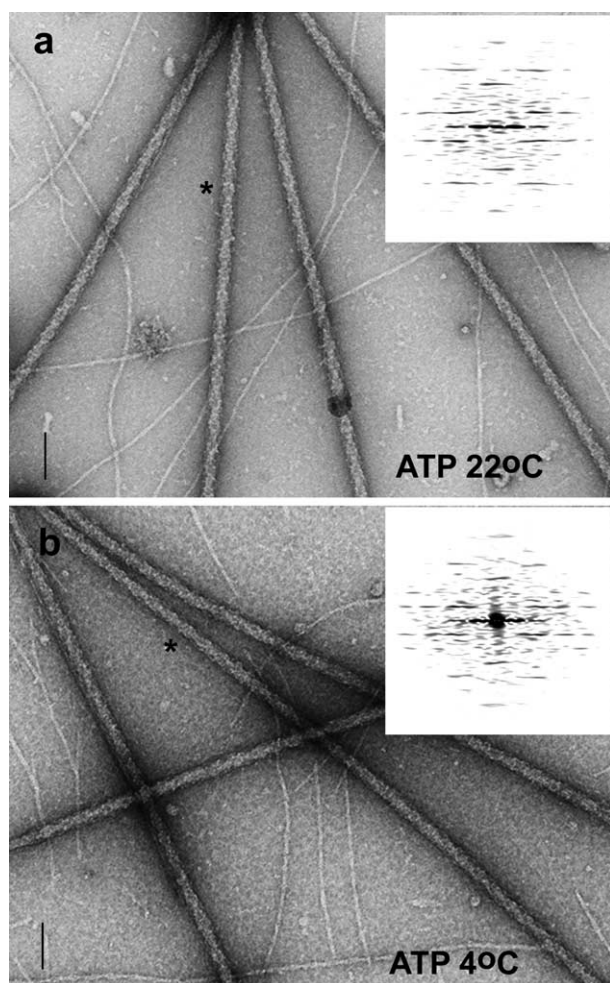


Figure 2. Tarantula thick filaments in relaxing conditions are helically ordered at 22 °C (a) and 4 °C (b). Asterisks here and in other Figures indicate the filament used to calculate the Fourier transform shown in the inset of each image. In both transforms, layer-lines indexing on the repeat of ~43 nm are evident. Scale bars represent 100 nm.

possible to determine whether AMPPNP or ATP γ NH₂ could induce helical ordering of the myosin heads.

ADP.BeF_x, ADP.AIF₄ and ADP.Vi induced helical order at both 22 °C and 4 °C

ADP, like AMPPNP and ATP γ NH₂, did not dissociate filaments (Figure 4a). However, a dramatically different result was obtained if ADP was accompanied by either Vi, or NaF plus BeCl₂ or AlCl₃. Formation of the complexes ADP.Vi, ADP.BeF_x and ADP.AIF₄ resulted in dissociation of the thick from the thin filaments similar to that observed with ATP (Figure 4b–d). In all cases the thick filaments were helically ordered at both 22 °C and 4 °C, evident both visually and by the appearance of strong layer-lines in their respective Fourier transforms. Thus, tarantula thick filaments can be

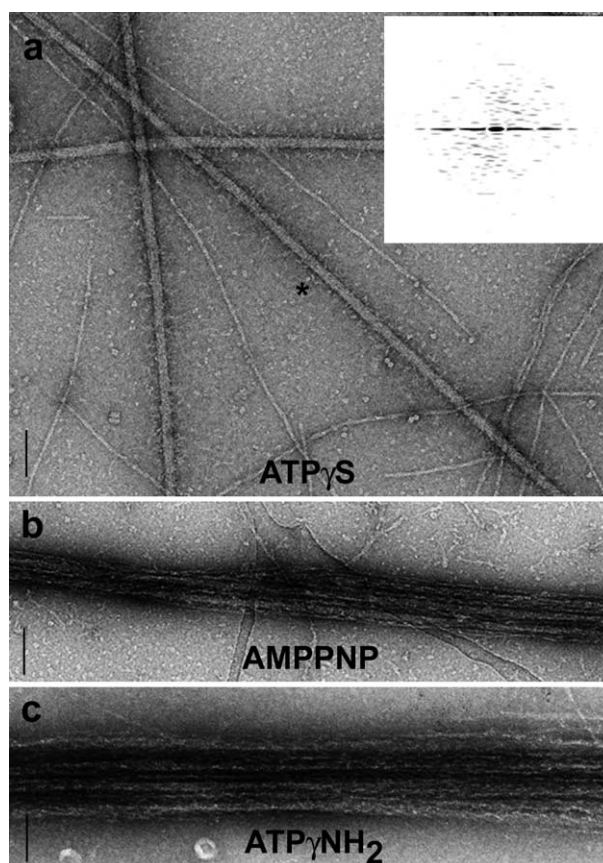


Figure 3. Analogs of ATP produced different effects on thick filament structure. ATP γ S caused dissociation but not ordering, as was evident both by eye and by the absence of helical layer-lines in the Fourier transform (a). Neither AMPPNP (b) nor ATP γ NH₂ (c) dissociated filaments. Scale bars represent 100 nm.

helically ordered by ADP.AIF₄ and ADP.Vi (ADP.Pi analogs) and also by ADP.BeF_x (an ATP analog).

Purified thick filaments can be used to study the effect of analogs that do not induce dissociation

Although most of the studied nucleotides dissociated the thick and thin filaments, ADP, AMPPNP and ATP γ NH₂ did not. It was therefore not possible to determine if these nucleotides could induce helical order in the thick filaments because the myosin heads remained bound to the thin filaments. Prior dissociation of thick from thin filaments,³⁰ is an alternative way to study the effect of these analogs on thick filament structure. This purification method requires ATP (relaxing solution) to initially dissociate the thick and thin filaments, and the ATP must then be completely removed for the effect of the added nucleotide to be determined (see Materials and Methods). Purified thick filaments in rigor conditions were visually disordered (Figure 5a), and this was confirmed by the extreme weakness of helical layer-lines in the

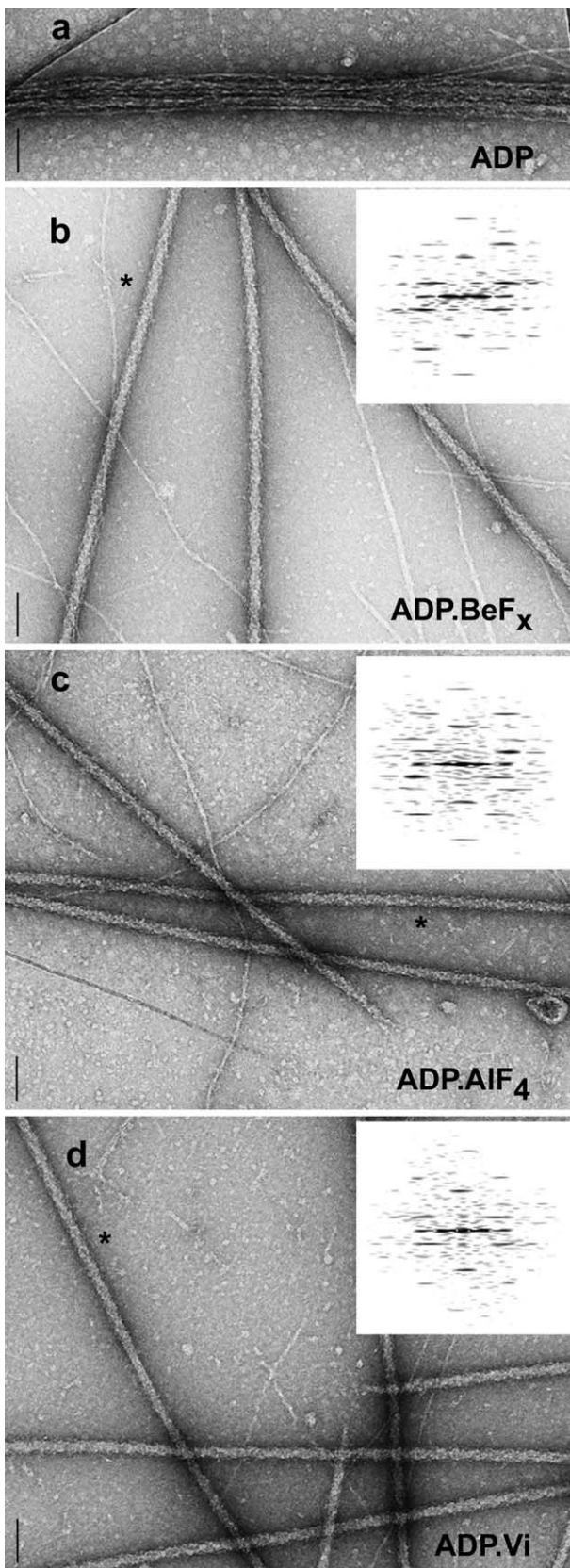


Figure 4. ADP did not induce dissociation of thick from thin filaments (a), while ADP.BeF_x (b), ADP.AlF₄ (c) and ADP.Vi (d) all induced dissociation and helical ordering of thick filaments with strong helical layer-lines in Fourier transforms (insets in b–d). Scale bars represent 100 nm.

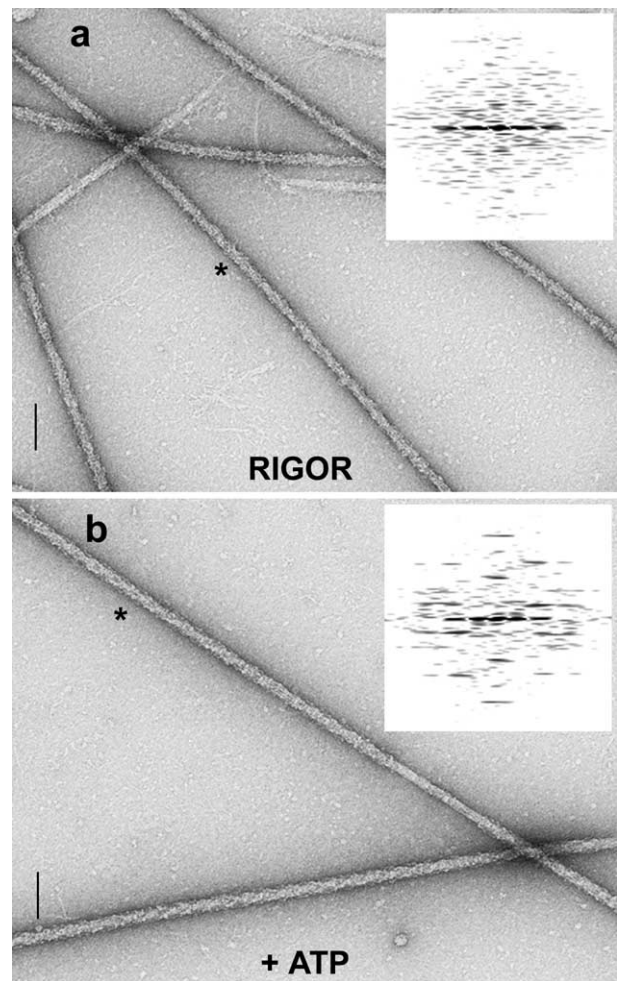


Figure 5. Purified thick filaments in rigor appear disordered (a), and this was confirmed by the Fourier transform (inset). Addition of ATP to these filaments caused helical ordering (b), and strong layer-lines with helical information appear in the Fourier transform. Scale bars represent 100 nm.

Fourier transform. The transforms were noisier than those obtained from ordered filaments and only weak meridional reflections were occasionally observed. Addition of ATP to such filaments induced helical re-ordering comparable to that seen in ATP-dissociated myofibrils (compare Figures 1b and 5b). Helical order is evident by the strong layer-lines in the Fourier transform. Thus, we used this preparation to determine if ADP, AMPPNP or ATP γ NH₂ induced helical order.

AMPPNP and ATP γ NH₂ but not ADP induced helical order in purified thick filaments

While ADP, AMPPNP and ATP γ NH₂ all gave the same result in myofibrils (no dissociation), they gave differing results with purified filaments (Figure 6). After addition of ADP (Figure 6a) the filaments were not obviously different from filaments in rigor. On the other hand, AMPPNP and

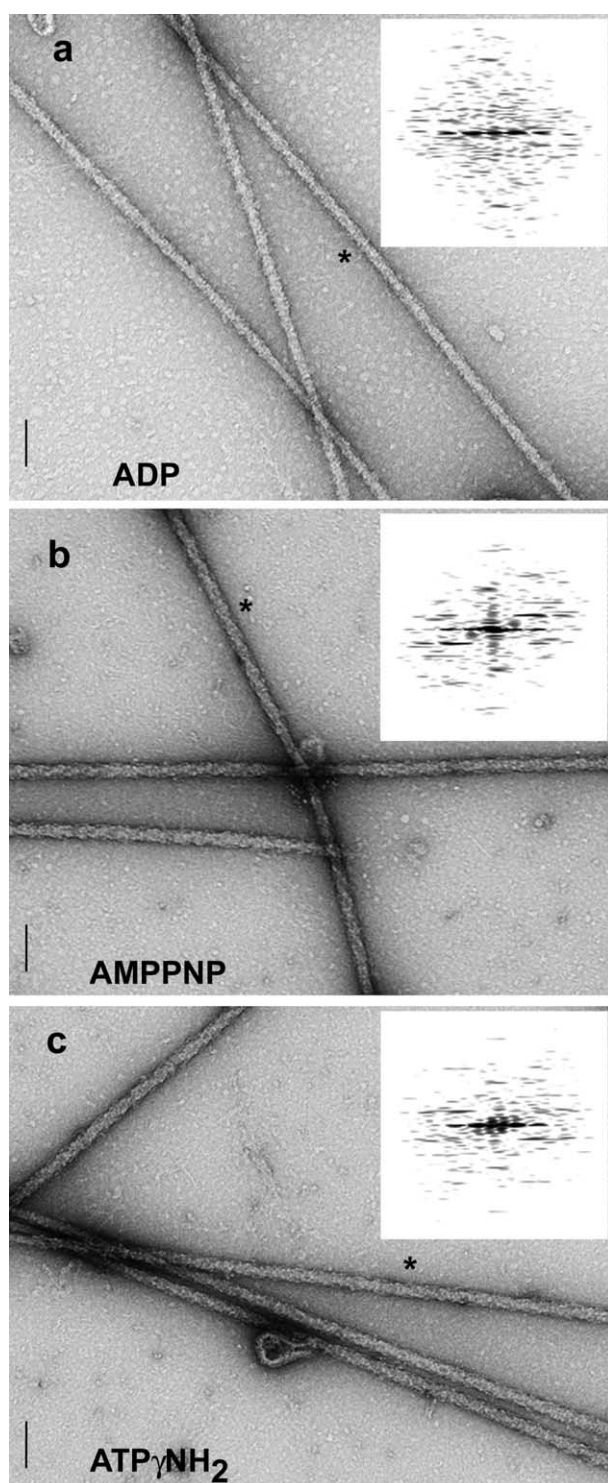


Figure 6. Purified thick filaments in the presence of ADP were disordered (a), with no obvious helical layer-lines (inset). In contrast, AMPPNP (b) and $\text{ATP}\gamma\text{NH}_2$ (c) induced helical order in purified filaments, and this was confirmed by the presence of helical layer-lines in their transforms. Scale bars represent 100 nm.

$\text{ATP}\gamma\text{NH}_2$ induced helical ordering, at both 22 °C (Figure 6b and c, respectively) and 4 °C (not shown). Thus, these two ATP analogs also induce helical order.

Comparison of helical order in tarantula thick filaments exposed to different nucleotides and temperatures

To compare the degree of ordering of the helices induced by different temperatures and analogs, we calculated average Fourier transforms from 20 equal-length segments of the best-ordered examples of each condition. The relative degrees of helical order were determined by visual inspection of the averaged transforms (Figure 7) and by comparing their vertical profiles (the integrated intensities of the layer-lines projected onto a line parallel to the meridian). These vertical profiles are shown to the right of each averaged transform. Based on these criteria, ATP-dissociated filaments at 22 °C showed the best order (Figure 7a), in agreement with the apparent order seen in the filament images. Strong layer-lines were also seen in ATP filaments at 4 °C, although in vertical profile they appeared weaker than at 22 °C (Figure 7b), suggesting a small effect of temperature on helical order. In rigor, most filaments showed no order. In the few partially ordered filaments that were found, the layer-lines were very weak and occurred mainly on the meridian of the third and sixth layer-lines (Figure 7c). The averaged transforms and vertical profiles for those analogs that induced helical order showed strong layer-line peaks and were very similar both between analogs, and with the same analog at 22 °C and 4 °C. Thus, only those calculated for filaments at 22 °C are shown (Figure 7d–h).

For a quantitative comparison of the helical order we analyzed the horizontal profile of the first myosin layer-line of each averaged Fourier transform (see Materials and Methods, Figure 10d and Xu *et al.*¹⁹). The area under each profile provides an indication of the helical order in each condition, greater area implying better order. Areas (Table 1) for $\text{ADP}\cdot\text{AlF}_4$, $\text{ADP}\cdot\text{Vi}$, $\text{ADP}\cdot\text{BeF}_x$, and $\text{ATP}\gamma\text{NH}_2$ were not significantly different from ATP or from each other ($p > 0.05$), suggesting a similar helical order with ATP and these analogs. However, AMPPNP induced a significantly poorer helical order than ATP and $\text{ADP}\cdot\text{AlF}_4$ ($p < 0.05$). In the presence of ATP, the helical order at 4 °C was significantly less than at 22 °C, whereas in the presence of analogs the helical order was not significantly affected by temperature. Thus, lower temperature appears to affect only the helical order induced by ATP. These area measurements suggest that at 4 °C helical order induced by ATP was poorer than helical order induced by $\text{ADP}\cdot\text{AlF}_4$, $\text{ADP}\cdot\text{Vi}$, and $\text{ADP}\cdot\text{BeF}_x$, and similar to helical order induced by AMPPNP and $\text{ATP}\gamma\text{NH}_2$.

Discussion

Our results show that helical ordering of the myosin heads is induced by analogs of both ATP ($\text{ADP}\cdot\text{BeF}_x$, AMPPNP, and $\text{ATP}\gamma\text{NH}_2$) and ADP·Pi ($\text{ADP}\cdot\text{AlF}_4$ and $\text{ADP}\cdot\text{Vi}$), but not by ADP, $\text{ATP}\gamma\text{S}$, or

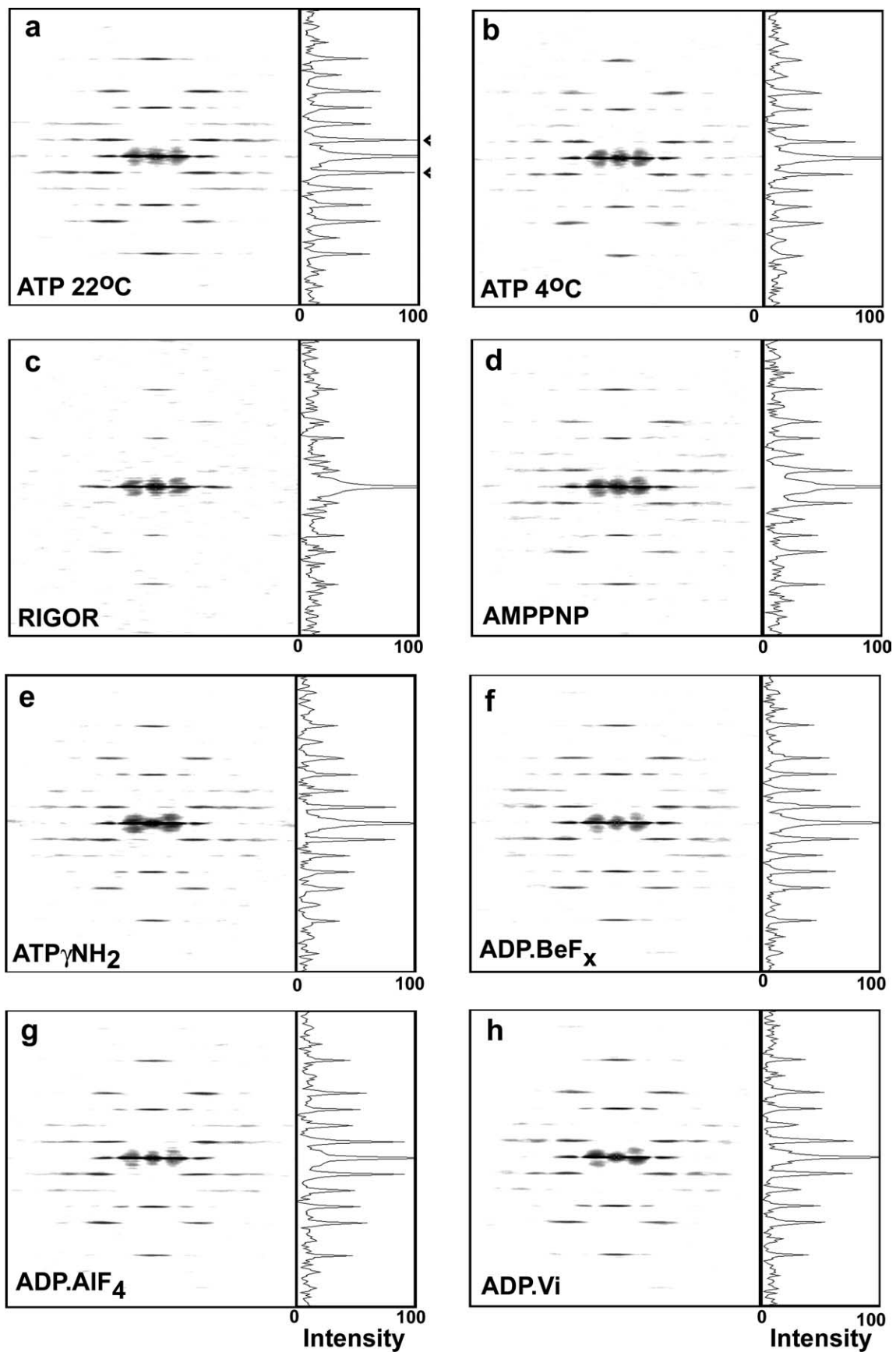


Figure 7. Averaged transforms calculated from filaments under different conditions, together with their vertical profiles calculated by projecting density onto the ordinate (at right of each transform, intensity in arbitrary units). Strong layer-lines are clearly visible in the presence of ATP at both 22 °C (a) and 4 °C (b). The profile in a was scaled so that the

Table 1. Area ($\text{pixel}^2 \times 10^2$) of the first myosin layer-line (mean \pm standard error, $n=20$) measured between $1/20 \text{ nm}^{-1}$ and $1/5 \text{ nm}^{-1}$ (Figure 10d) for the different analogs that induce helical order at 22 °C and 4 °C

| Analog | 22 °C | 4 °C | 4 °C/22 °C |
|------------------------------|--------------|--------------|------------|
| ATP | 129 \pm 13 | 97 \pm 4 | 0.75* |
| ADP.AIF ₄ | 119 \pm 10 | 124 \pm 13 | 1.04 |
| ADP.Vi | 113 \pm 17 | 113 \pm 8 | 1.00 |
| ADP.BeF _x | 110 \pm 21 | 116 \pm 10 | 1.05 |
| ATP γ NH ₂ | 107 \pm 11 | 117 \pm 15 | 1.09 |
| AMPPNP | 91 \pm 3 | 99 \pm 7 | 1.09 |

The column 4 °C/22 °C shows the effect of temperature for each analog and the asterisk indicates that for ATP the effect was statistically significant ($p < 0.05$).

the absence of nucleotide. We conclude that ATP hydrolysis is not a requirement for helix formation, contrary to the previous hypothesis that the bound ATP had to be in the ADP.Pi state.^{18,19} As discussed below, the conformation of the myosin head, rather than the state of the bound nucleotide, appears to be the key determinant of helix formation.

Helical order requires the “closed” conformation of the myosin head

Myosin heads from different species have been crystallized in three globally different conformations. An “open” conformation (with the γ phosphate pocket open, and the lever arm “down” at an angle of approximately 45° to the thin filament axis) has been reported for heads in the absence of nucleotide, in the presence of ADP, AMPPNP, ATP γ S, and ADP.BeF_x, and also in the presence of ATP in a head unable to hydrolyze it.^{31–35} A “closed” conformation (with the γ phosphate pocket closed, and the lever arm “up” approximately perpendicular to the thin filament axis) has been reported with ADP.AIF₄, ADP.Vi and ADP.BeF_x.^{32,34,36,37} A third conformation called the “detached” conformation (with the γ phosphate pocket open, and the lever arm close to and almost parallel to the thin filament axis) has been reported only in scallop myosin crystallized in the presence of ADP, ADPBeF_x, AMPPNP, or ATP γ S.^{38,39} In these structures, the closure or opening of the γ phosphate pocket is determined by the positioning of switch 2 either near to or away from the nucleotide, respectively.^{26–28} The closed or open notation for the myosin head is frequently used to denote the

closing or opening of switch 2, and thus of the nucleotide pocket.

In addition to this crystallographic information, dynamic experiments have been carried out in the presence of different analogs in solution, using the intrinsic tryptophan fluorescence of the myosin head as an indicator of head conformation (greater fluorescence corresponding to a closed conformation).^{40–42} These experiments have shown that there is an equilibrium between the open and closed conformations that depends on the nucleotide and/or the temperature.⁴¹ It is therefore not surprising⁴⁰ that the same analog (for example, ADP.BeF_x) can induce both the open³² and the closed conformation³⁷ in crystallographic studies. However, most of the available crystallographic studies (see above) have trapped just one of the conformations (presumably that favored by the crystallization conditions employed).

Intrinsic fluorescence of nucleotide-free *Dictyostelium* myosin increases in the presence of ATP and ADP.AIF₄, and also in the presence of ADP.BeF_x and AMPPNP (but only at temperatures higher than 20 °C).⁴¹ This suggests that the open/closed transition is temperature-dependent and does not require the hydrolysis reaction.⁴¹ In a similar way, ATP γ NH₂ seems to stabilize the closed conformation in rabbit myosin without being hydrolyzed.⁴² Concomitantly, every analog that has been shown to induce the closed conformation of the myosin head also induces helical order in tarantula thick filaments, while those that promote the open conformation fail to induce order (Table 2). Thus, while helix formation does not require the hydrolysis reaction, it does appear to require that the myosin head adopts the closed conformation. Therefore, a slower hydrolytic step is not the cause of decreased helical order in thick filaments at low temperature as was previously suggested.^{18, 20, 22} Instead, because the closed conformation appears to be necessary for the hydrolysis of ATP,^{26,35,36} the slower hydrolytic step may be a consequence of the less favorable transition to the closed conformation at low temperature.^{40–42}

During the course of this work, an X-ray diffraction study of helical ordering in rabbit muscle filaments in the presence of ATP analogs was reported.⁴³ Helical order was found in the presence of ADP.Vi, AMPPNP, ADP.BeF_x and ADP.AIF₄, but only at temperatures higher than 20 °C. Myosin heads were disordered with ADP or ATP γ S, or in the absence of nucleotide at all temperatures. The ability of each analog to promote helical order at

intensity of the first layer-line (arrowheads) was arbitrarily assigned a value of 100. All other profiles were scaled by the same factor, so that the peak intensities between the different profiles are directly comparable. Averaged transforms and their vertical profiles for filaments at 22 °C are shown for filaments in rigor (c) and in the presence of different analogs that induced helical order: AMPPNP (d); ATP γ NH₂ (e); ADP.BeF_x (f); ADP.AIF₄ (g); ADP.Vi (h). Twenty equal-length filament segments were used to calculate each averaged transform, except for rigor, where only ten usable segments were found (these were the only ones showing any clear reflections on the third and sixth layer-lines, which were necessary for the spatial scaling of the transforms required for averaging). Because disordered filaments (the majority) could not be included in the rigor average, the true degree of helical order in rigor will be considerably less than that suggested by the transform in c.

Table 2. The ability of the analogs to induce helical order observed in negatively stained thick filaments was related to their ability to induce the closed conformation of the myosin head according to crystallographic or intrinsic tryptophan fluorescence studies

| Analog | Helical order | Myosin head conformation | |
|------------------------------|---------------|-----------------------------------------------------|-------------------------------------|
| | | Crystallography | Fluorescence |
| No nucleotide | No | O ^{31,34} | O ⁴⁰ |
| ATP | Yes | O ³⁵ (un-hydrolyzed ATP) | C ⁴⁰ |
| ADP | No | O ³³ ; D ^{38,39} (cross-linked) | O ^{40,41} |
| ATP γ S | No | O ³³ ; D ³⁹ (cross-linked) | O ⁴⁰ |
| AMPPNP | Yes | O ³³ ; D ³⁹ | C ^{40,41} (at $T > 20$ °C) |
| ATP γ NH ₂ | Yes | Not crystallized yet | C ⁴² |
| ADP.BeF _x | Yes | C ³⁷ ; O ³² ; D ³⁹ | C ⁴⁰ (at $T > 20$ °C) |
| ADP.AIF ₄ | Yes | C ^{32,37} | C ^{40,41} |
| ADP.Vi | Yes | C ^{34,36} | Not studied ⁴⁰ |

O, open conformation; C, closed conformation; D, detached conformation.

different temperatures was found to be similar to its ability to promote the closed conformation,^{40–42} and these authors therefore concluded that helical order requires the closed conformation of the head.⁴³ In general, our data support these observations on rabbit filaments at 20 °C, but we find that these same analogs induce helical order in tarantula filaments at lower temperature as well. Quantitative analysis showed that in the presence of ATP the integrated intensity of the first myosin layer-line was only 25% smaller at 4 °C than at 22 °C (Table 1). This effect of temperature on helical order appears small compared to that in rabbit^{22,25} or chicken thick filaments.²¹ We also found no such temperature effect with any other nucleotide. These results suggest a small temperature dependence for the open to closed transition in tarantula myosin, which might also occur in myosin from other cold-blooded animals whose thick filaments are well ordered in the relaxed state at low temperature (like frog and fish^{23–25}). In support of this view, the existence of helical order in frog muscle with ADP.Vi at 5 °C⁴⁴ suggests that this analog may also promote the closed conformation in frog myosin at low temperature (in contrast to the open conformation favored in rabbit under similar conditions⁴³). It thus appears that the requirement of the closed conformation for helical ordering is common to both invertebrate and vertebrate thick filaments, whether or not they are temperature-dependent. Favoring of the closed conformation and thus of helical ordering of myosin heads in all species at their normal temperature of operation (homeotherms at high temperatures, and poikilotherms at both high and low temperatures) suggests that this ordering is a key feature of the relaxed state. It may be essential to efficient energy conservation in relaxed muscle (by minimizing thick–thin filament interaction) and to the efficient switching on of contraction.

Further evidence that the closed conformation underlies the helically ordered state comes from fitting the atomic structure of the chicken myosin head (in the absence of nucleotide³¹) to the 3D reconstruction of the tarantula filament.^{8,14} Using

this atomic structure (which is in the open conformation³¹), the initial fit was poor, but this was improved when the head was allowed to flex, producing a structure more similar to the closed conformation.¹⁴ This independently suggests that helical order cannot be established when the myosin heads are in the open conformation, and that a molecular shape similar to the closed conformation is required. A similar conclusion was obtained for the thick filaments of relaxed insect flight muscle⁵ where optimal modeling of the X-ray pattern of the relaxed muscle was obtained with a modification of the open conformation³¹ whose final molecular shape was similar to the closed conformation.³⁴ The one exception to this conclusion comes from X-ray modeling of fish muscle, in which it was concluded that resting myosin heads had a shape similar to the nucleotide-free³¹ shape.⁴ Since ADP.Pi was expected to be the predominant nucleotide species under the conditions of this study, it was suggested that the structure of the myosin head in the absence of nucleotide must be very similar to that observed in the presence of ADP.Pi.⁴ However, this conclusion does not appear to be supported by crystallographic data obtained after this study, showing that ADP.Pi heads have a different shape from those without nucleotide.^{31,32,34–37} It would be interesting to determine if a similar modeling for the fish thick filaments, but using a closed conformation of the myosin head as starting shape, might result in a better fit of the X-ray diffraction data.

Insight into how the closed conformation generates helical ordering of the heads may come from fitting the closed atomic structure^{32,34,37} to the 3D reconstruction of frozen-hydrated tarantula filaments currently in progress (R.P., L. Alamo & R.C., unpublished results). Such an atomic model may reveal the intra- or intermolecular interactions involved in generating helical order. For example, in the closed conformation some regions of the essential light chain are much closer to the active site than in the open conformation.^{26,31,36} This type of intra-molecular interaction (between regulatory and motor domain, for example) and the

interactions between neighboring heads⁴⁵ could be important in thick filament regulation.

Different nucleotides produce the same helical structure

Although nucleotides favoring the closed conformation generate helical ordering of the heads, we have not shown whether the helical structure is the same for each nucleotide. We assume that the heads in all cases originate at the same helical points on the thick filament backbone (determined by the packing of the myosin tails), but we do not know whether the orientation or interactions of heads change with different nucleotides. While the most detailed comparison between structures would be achieved by comparing their full 3D reconstructions,⁸ a simple approximation can be made by comparing the averaged Fourier transforms and filtered images obtained under each condition. Visual comparison of the transforms (Figure 7) shows similar relative intensities and positions of reflections in all the conditions that produce helical order, suggesting similar thick filament structures. More quantitatively, the distance between the meridional reflection and its first subsidiary on the third layer-line was the same for all the helically ordered filaments, regardless of analog or temperature. This implies that the average radial position of the center of mass of the helically ordered heads³ is similar in all the conditions studied.

Additional information on the helical organization in different conditions can be gained by helical filtering of the filament images. Filtering enhances the helical structure (by removing non-helical information) and can be used to separate information coming from the two sides of the filament, providing a visual image of the helical tracks on one side without interference from the other.⁴⁶ Figure 8a shows a one-sided filtered image of a representative thick filament in ATP at 22 °C. The subunit shape and organization are similar to those in a one-sided longitudinal projection of the full 3D reconstruction of the tarantula filament⁸ (L. Alamo, personal communication). This confirms that the simple filtering procedure provides a valid indication of the subunit organization on these filaments. Filaments with a high degree of helical order (higher peak areas in Table 1) revealed strong helical tracks along the thick filament (e.g. ATP at 22 °C (Figure 8a) or ADP.AIF₄ (Figure 8b)). Less favorable conditions, such as AMPPNP (Figure 8c) or ATP at 4 °C, showed weaker helical tracks. In these cases, the weaker helical ordering appears to result from patches of filament that are well ordered (with a similar structure in all cases) combined with patches that exhibit less order, rather than from a homogeneous distribution of a different helical structure. In rigor, helical tracks were essentially absent (Figure 8d). The subunit shape and organization in the filtered images were similar in all the ordered filaments studied, supporting the conclusion (from comparison of the transforms)

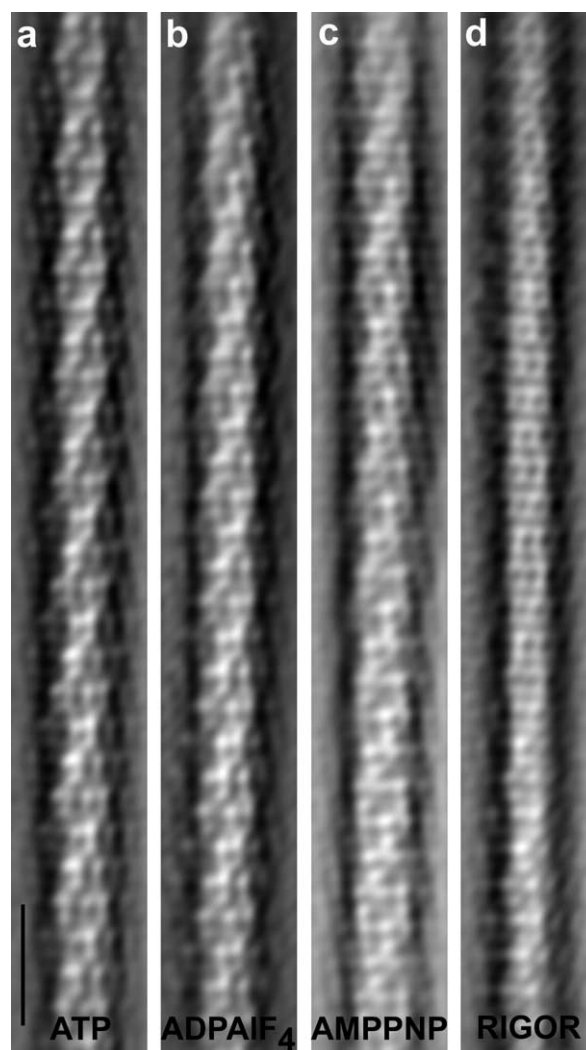


Figure 8. One-sided image filtrations obtained under four representative conditions: a, ATP; b, ADP.AIF₄; c, AMPPNP and d, rigor, all at 22 °C. Helical order decreases from left to right. Filaments with ATP and ADP.AIF₄ show strong helical tracks with a subunit shape and organization that resembles the atomic model for the tarantula thick filament.¹⁴ The filament with AMPPNP shows similar helical tracks, although weaker. Scale bar represents 50 nm.

that different nucleotides do not significantly alter the orientations or interactions of helically ordered heads.

Implications for muscle physiology

We have concluded that in relaxed muscle a high proportion of myosin heads are in the closed conformation, forming helices on the thick filament surface. Because the closed conformation is the pre-power stroke state,²⁶ the heads in relaxed muscle are ready to produce force. Ordering of the heads near the thick filament backbone might be an important mechanism for reducing the probability of interactions with thin filaments in relaxing

conditions (in addition to regulation by the thin filament). The possible importance of sequestering heads away from the thin filament in relaxed muscle becomes clear when one considers the dimensions of the filament lattice. In tarantula muscle, each thick filament in the overlap region is surrounded by 9 to 12 regularly distributed thin filaments⁷ (Figure 9). In the live state, the thick filaments form a hexagonal lattice with a center-to-center distance of 58 nm (based on X-ray diffraction).^{47,48} If the thin filaments lie approximately midway between the thick filaments, the center-to-center distance between thick and thin filaments will be ~29 nm. With thin and thick filament (backbone) radii of ~5 nm⁴⁹ and ~10 nm,⁸ respectively, the distance between their surfaces would be only ~14 nm. This distance is shorter than the length of the myosin head,³¹ which could make it easy for myosin heads to contact actin. However, the diameter of relaxed, helically ordered tarantula thick filaments to the outer edges of the myosin heads is 38 nm (based on measurements of frozen hydrated filaments; L. Alamo, R. Horowitz, F. Q. Zhao, R.C. & R.P., unpublished results). The compact ordering of the heads implied by this measurement would thus maintain a gap of ~5 nm between filament surfaces (Figure 9). This may function to minimize thick–thin filament interaction (and therefore ATP usage), and thus help to maintain the relaxed state. Maintaining a gap between filament surfaces may also be important in minimizing resistance to stretch that occurs when antagonist muscles contract (cf. Xu *et al.*⁴³). Similar calculations, combining published interfilament distances and estimates of thick filament diameter,^{1,50–55} suggest that a comparable gap occurs in a variety of muscles having different lattices and thick filament structures. Modeling of muscle X-ray patterns suggests that in some cases this gap may

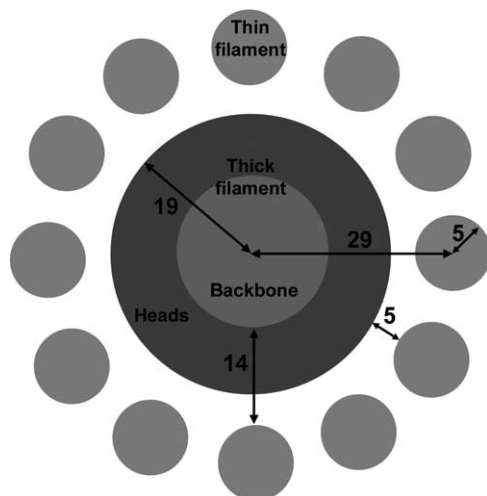


Figure 9. Diagram showing diameters and distances (in nm) between thin and thick filaments in the filament lattice of live tarantula muscle. In the thick filament, the dark annulus represents the volume occupied by the heads. See details in the text.

be very small (1–2 nm^{4,5,52}). Ordering of heads in the relaxed state may thus play a similar role in many muscles.

In summary, our electron microscopic observations directly relate the atomic structure of the myosin head as determined by X-ray crystallography to the head conformation present in the native filament. We conclude that the closed conformation of the myosin head is the key requirement for the ordering of the heads into helical paths on the filament surface. This may play an important role in the energetics and mechanics of relaxed muscle.

Materials and Methods

Solutions

(1) Rigor solution is 100 mM sodium chloride, 3 mM magnesium chloride, 1 mM EGTA, 5 mM Pipes, 1 mM sodium azide (pH 7.0). (2) Relaxing solution is rigor solution plus 5 mM MgATP (pH 7.0). (3) Analog solution is rigor solution plus 5 mM MgAnalog (pH 7.0). Analog solutions also contained hexokinase and glucose as detailed below under Treatment with nucleotides. (4) Rigor rinse solution is 100 mM sodium acetate, 1 mM magnesium acetate, 1 mM EGTA, 5 mM imidazole, 1 mM sodium azide (pH 7.0) (see more details below under Electron microscopy). (5) Vanadate (Vi) stock solution was made as described by Goodno.⁵⁶

Specimen preparation

Myofibrils

Rigor myofibrils were obtained from tarantula leg muscles (*Brachypelma* sp and *Avicularia avicularia*; Carolina Biological Supply, USA) in a similar way to that described for thick filaments,⁴⁵ only using rigor solution instead of relaxing solution in all procedures. Briefly, muscles were permeabilized for three hours in rigor solution plus saponin (0.1%, w/v) and then rinsed at least twice with rigor solution (the first overnight). Skinned muscles were homogenized in rigor solution and the homogenate spun for ten seconds at 6000g to remove large debris. The supernatant contained a suspension of myofibrils in rigor. All procedures were carried out at 4 °C.

Purified thick filaments

Some analogs did not induce dissociation of thick and thin filaments when added to myofibrils. In these cases a thick filament suspension previously dissociated from thin filaments was used to study the effect of these analogs on thick filament structure. Following dissociation, thick filaments were purified using calcium-insensitive gelsolin to remove the thin filaments.³⁰ The filament suspension was then centrifuged for 15 minutes at 18,000g. Pellets were resuspended and incubated two hours at room temperature in rigor solution (pH 6.5) containing hexokinase (1 mg/ml) and glucose (1 mM) to remove residual ATP⁵⁷ and AP₅A (1 mM) to inhibit endogenous adenylate kinase.⁵⁸ The suspensions were then centrifuged again for 15 minutes at 18,000g and the pellets resuspended in the desired solution (rigor, or

relaxing solution, or rigor plus the specific analog, pH 7.0).

Treatment with nucleotides

The nucleotides studied were ADP, the ATP analogs: ATP γ S,⁵⁹ AMPPNP,⁶⁰ ATP γ NH₂,⁴² and ADP.BeF_x,³² and the ADP.Pi analogs: ADP.AIF₄,^{32,61} and ADP.Vi.^{36,56,62} ATP, ADP, ATP γ S, AMPPNP and NaF were purchased from Sigma, BeCl₂ and AlCl₃ from Fluka, and sodium orthovanadate from Aldrich. ATP γ NH₂ was kindly donated by John Wray and Werner Jahn (Max Planck Institute, Germany). ATP contamination (0.1–0.8%) was detected in some analogs through the luciferin/luciferase bioluminescent assay (Sigma). This contamination could have significantly affected the results at the 5 mM concentration of analogs used. All solutions containing analogs were therefore treated for 20 minutes at room temperature with hexokinase (type IV, Sigma; 1 mg/ml) and glucose (1 mM) prior to use,⁵⁷ reducing ATP contamination below 100 nM according to the same assay. The inability of AMPPNP and ATP γ NH₂, even at high (30 mM) concentration, to dissociate thick and thin filaments, confirms that ATP contamination is effectively eliminated by this procedure (see Results). AP₅A⁵⁸ (Sigma) was also added to preparations prior to analog addition.

Myofibrils or purified thick filaments in rigor were incubated at least ten minutes at room temperature or 4 °C prior to analog addition. ATP or analogs (rigor solution plus 5 mM Mg.Analog pretreated with hexokinase and glucose) were then added and the specimens maintained at their respective temperature. To form the complexes ADP.BeF_x, ADP.AIF₄ and ADP.Vi, 5 mM Mg.ADP was added to myofibrils, followed by 5 mM NaF and 1 mM BeCl₂, or 5 mM NaF and 1 mM AlCl₃ or 1 mM Vi, respectively.^{56,61–63}

Electron microscopy

Tarantula thick filaments were negatively stained with 1% uranyl acetate on holey carbon grids covered with an additional thin carbon layer floated from mica. Only filaments on the thin carbon over holes were studied. Staining was improved (1) by using relatively fresh (\leq one week old) thin carbon, which was picked up from the water surface just prior to applying the specimen; (2) by leaving a significant meniscus of stain on the grid before drying (i.e. not all stain was withdrawn); and (3) by drying the grids slowly in a humid atmosphere (\sim 80% R.H.). Specimens were rinsed with an acetate-based rinse prior to staining to prevent disruption of thick filament structure that can occur with high (0.1 M) chloride;^{8,13} imidazole was used as the buffer in these solutions as it appeared to improve the staining. An appropriate rinse solution was used for each case, rigor filaments being rinsed with rigor rinse, and nucleotide-treated filaments with rigor rinse containing 1 mM Mg.ATP or 1 mM of the respective analog pretreated with hexokinase and glucose. All specimens and solutions were pre-incubated at the appropriate temperature before staining. Filaments incubated at room temperature were stained at room temperature, and filaments incubated at 4 °C were stained in the cold room at 4 °C.

Grids were observed in a Philips CM-10 or CM-120 transmission electron microscope at 80 kV and normal electron dose. Micrographs were recorded on Kodak 4489 film.

Image processing

Digitization of filaments and computation of the fast Fourier transform

Micrograph negatives were digitized using a Panasonic Industrial CCD Camera (GP-MF-802) controlled by Scion Image v 4.0.2 (Scion Corporation). Segments of filaments containing ten helical repeats (435 nm for tarantula filaments) were digitized at \sim 9 Å/pixel and boxed in a 460 \times 60 pixel window with the bare zone located at the top of each image. The boxed image was floated in a 512 \times 512 pixel array, the box edges apodized and the fast Fourier transform computed. All image processing procedures were carried out using Scion Image.

Quantification of helical order

For a quantitative comparison of the helical order of the thick filaments at different temperatures and with different analogs, an averaged Fourier transform power spectrum computed from 20 of the best stained and best ordered filament segments was calculated for each condition. To calculate the average, each transform was spatially scaled using the third and sixth layer-line as reference, and ensuring that each layer-line lay on an integral number of pixels. Observable changes in the averaged transforms were minimal after ten filaments had been included. The use of 20 filaments therefore ensured that each average was an accurate representation of each state.

A vertical profile of each averaged transform was obtained by projecting the average intensity value along each horizontal line of pixels onto a line parallel to the meridian (Figure 10a and b, right). The background on the transform (Figure 10a) was subtracted using the rolling ball method (Figure 10b). The vertical profiles obtained after subtraction of the background were used to compare the overall helical information present under different conditions.

For quantification of helical order we calculated the integrated intensity of the first myosin layer-line (43.5 nm repeat, the helical track most obvious to the eye in the original micrographs). A similar procedure was used previously to quantify the degree of helical order of myosin heads in X-ray diffraction patterns.¹⁶ In order to measure this integrated intensity we obtained a horizontal profile of the first myosin layer-line (Figure 10c) using a slice 512 pixels long and three pixels wide of the averaged transform. In these horizontal profiles, the information extending laterally beyond 1/5 nm⁻¹ was considered to be noise. The base line was adjusted to coincide with the approximate mid-level of this noise, and the area above this base line measured between 1/20 nm⁻¹ and 1/5 nm⁻¹ on both sides of these horizontal profiles (Figure 10d). These limits select out primarily the J_4 Bessel function of the first layer-line of tarantula thick filaments.⁸ This area provides a measure of the degree of helical order of the myosin heads.

Statistical comparison of areas in different conditions was not possible by measuring individual transforms, owing to the poor signal-to-noise ratio. Areas could be measured, however, from averages of five filaments. For statistical comparison, the 20 filaments selected for each condition were therefore randomly distributed into four groups of five filaments, and four average transforms calculated. The averages were used to calculate a mean and standard error for each condition. Statistical

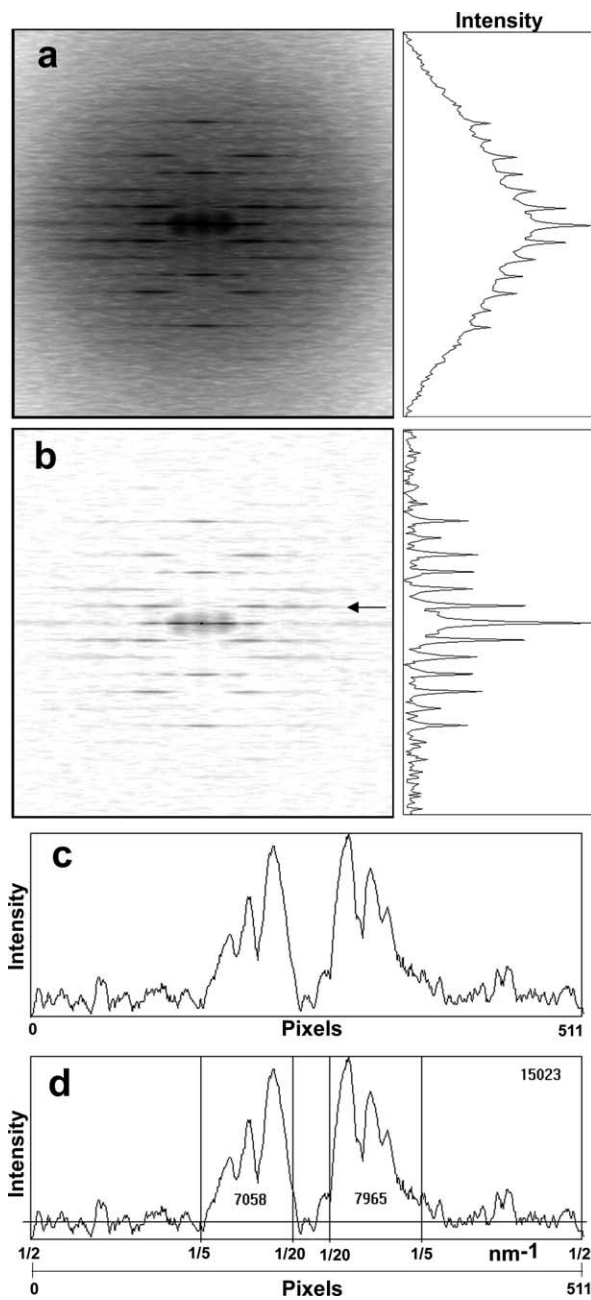


Figure 10. Analysis of Fourier transforms. The central part (256×256 pixels) of a raw average (512×512 pixels) and its vertical profile is shown in (a). Peaks with helical information lie on top of a high background. After background subtraction (b) the vertical profiles show the peaks above a straight base line. A horizontal profile in a 512×3 pixel window centered on the first layer-line (indicated by the arrow in b) is shown in c. This profile was used to measure the area of the first myosin layer-line above a base line drawn through the approximate mid-level of the noise (obtained from the profile extending laterally beyond $1/5 \text{ nm}^{-1}$) (d). Vertical lines (located at positions corresponding to $1/20 \text{ nm}^{-1}$ and $1/5 \text{ nm}^{-1}$ on both sides of the meridian) show the limits of the area measured (see Materials and Methods). Intensity is in arbitrary units.

comparison of the mean areas obtained under different conditions was carried out by the Student *t*-test.

Filtering

The Fourier transforms from representative filament images were layer-line filtered to provide a visual comparison of the head organization under different conditions. Interpretation of filtered images was facilitated by including information from only one side of the filament.⁴⁶ Selection of layer-lines (equator and layer-lines 1–6) coming from the back or front of the filament was made according to the previously published indexing of the diffraction pattern for tarantula thick filaments.⁸ In these filaments, some Bessel functions overlap even at low resolution.⁸ However, at the resolution of our filtering ($1/6.8 \text{ nm}^{-1}$ equatorially and $1/7.2 \text{ nm}^{-1}$ meridionally) the overlapping of Bessel functions (i.e. J_4 and J_8) is small,⁸ and does not have a significant impact on the filtered image.⁴⁶ This was clear from the close similarity of such a one-sided filtered image of a filament in ATP (relaxing solution) to a one-sided projection of the 3D reconstruction⁸ of tarantula filaments, where Bessel function separation had been carried out (L. Alamo, personal communication; data not shown).

Acknowledgements

We thank Lorenzo Alamo for discussion and for providing a one-sided filtered image of the 3D reconstruction of the tarantula thick filament. We thank John Wray and Werner Jahn for the gift of $\text{ATP}\gamma\text{NH}_2$. This work was supported by a grant from the Venezuelan National Fund for Science, Technology and Innovation (FONACIT) (to R.P.) and grants from the NIH (AR34711, HL62468 to R.C.). The research of R.P. was supported in part by an International Research Scholars grant from the Howard Hughes Medical Institute. M.E.Z. was the recipient of a fellowship from FONACIT during the years 1999–2003 and this work was part of her PhD thesis.⁶⁴ Electron microscopy was carried out at the Core Electron Microscopy Facility of the University of Massachusetts Medical School, supported in part by Diabetes Endocrinology Research Center grant DK32520. The contents of this paper are solely the responsibility of the authors and do not necessarily represent the official views of the granting agencies.

References

1. Huxley, H. E. (1968). Structural difference between resting and rigor muscle; evidence from intensity changes in the low angle equatorial X-ray diagram. *J. Mol. Biol.* **37**, 507–520.
2. Huxley, H. E. & Brown, W. (1967). The low-angle X-ray diagram of vertebrate striated muscle and its behavior during contraction and rigor. *J. Mol. Biol.* **30**, 383–434.
3. Wray, J. S., Vibert, P. J. & Cohen, C. (1975). Diversity of cross-bridge configurations in invertebrate muscles. *Nature*, **257**, 561–564.

4. Hudson, L., Harford, J. J., Denny, R. C. & Squire, J. M. (1997). Myosin head configuration in relaxed fish muscle: resting state myosin heads must swing axially by up to 150 Å or turn upside down to reach rigor. *J. Mol. Biol.* **273**, 440–455.
5. AL Khayat, H. A., Hudson, L., Reedy, M. K., Irving, T. C. & Squire, J. M. (2003). Myosin head configuration in relaxed insect flight muscle: X-ray modeled resting cross-bridges in a pre-powerstroke state are poised for actin binding. *Biophys. J.* **85**, 1063–1079.
6. Stewart, M., Kensler, R. W. & Levine, R. J. (1981). Structure of *Limulus* telson muscle thick filaments. *J. Mol. Biol.* **153**, 781–790.
7. Levine, R. J., Kensler, R. W., Reedy, M. C., Hofmann, W. & King, H. A. (1983). Structure and paramyosin content of tarantula thick filaments. *J. Cell Biol.* **97**, 186–195.
8. Crowther, R. A., Padrón, R. & Craig, R. (1985). Arrangement of the heads of myosin in relaxed thick filaments from tarantula muscle. *J. Mol. Biol.* **184**, 429–439.
9. Vibert, P. & Craig, R. (1983). Electron microscopy and image analysis of myosin filaments from scallop striated muscle. *J. Mol. Biol.* **165**, 303–320.
10. Stewart, M., Kensler, R. W. & Levine, R. J. (1985). Three-dimensional reconstruction of thick filaments from *Limulus* and scorpion muscle. *J. Cell Biol.* **101**, 402–411.
11. Stewart, M. & Kensler, R. W. (1986). Arrangement of myosin heads in relaxed thick filaments from frog skeletal muscle. *J. Mol. Biol.* **192**, 831–851.
12. Morris, E. P., Squire, J. M. & Fuller, G. W. (1991). The 4-stranded helical arrangement of myosin heads on insect (*Lethocerus*) flight muscle thick filaments. *J. Struct. Biol.* **107**, 237–249.
13. Eakins, F., AL Khayat, H. A., Kensler, R. W., Morris, E. P. & Squire, J. M. (2002). 3D Structure of fish muscle myosin filaments. *J. Struct. Biol.* **137**, 154–163.
14. Offer, G., Knight, P. J., Burgess, S. A., Alamo, L. & Padrón, R. (2000). A new model for the surface arrangement of myosin molecules in tarantula thick filaments. *J. Mol. Biol.* **298**, 239–260.
15. Haselgrove, J. C. (1975). X-ray evidence for conformational changes in the myosin filaments of vertebrate striated muscle. *J. Mol. Biol.* **92**, 113–143.
16. Padrón, R. & Craig, R. (1989). Disorder induced in nonoverlap myosin cross-bridges by loss of adenosine triphosphate. *Biophys. J.* **56**, 927–933.
17. Clarke, M. L., Hofman, W. & Wray, J. S. (1986). ATP binding and crossbridge structure in muscle. *J. Mol. Biol.* **191**, 581–585.
18. Wray, J. (1987). Structure of relaxed myosin filaments in relation to nucleotide state in vertebrate skeletal muscle. *J. Muscle Res. Cell Motil.* **8**, 62.
19. Xu, S., Gu, J., Rhodes, T., Belknap, B., Rosenbaum, G. Offer, G. *et al.* (1999). The M.ADP.P(i) state is required for helical order in the thick filaments of skeletal muscle. *Biophys. J.* **77**, 2665–2676.
20. Wakabayashi, T., Akiba, T., Hirose, K., Tomioka, A., Tokunaga, M., Suzuki, M. *et al.* (1988). Temperature-induced change of thick filament and location of the functional sites of myosin. *Advan. Expt. Med. Biol.* **226**, 39–48.
21. Kensler, R. W. & Woodhead, J. L. (1995). The chicken muscle thick filament: temperature and the relaxed cross-bridge arrangement. *J. Muscle Res. Cell Motil.* **16**, 79–90.
22. Malinchik, S., Xu, S. & Yu, L. C. (1997). Temperature-induced structural changes in the myosin thick filament of skinned rabbit psoas muscle. *Biophys. J.* **73**, 2304–2312.
23. Xu, S. G., Kress, M. & Huxley, H. E. (1987). X-ray diffraction studies of the structural state of cross-bridges in skinned frog sartorius muscle at low ionic strength. *J. Muscle Res. Cell Motil.* **8**, 39–54.
24. Harford, J. J. & Squire, J. M. (1992). Evidence for structurally different attached states of myosin cross-bridges on actin during contraction of fish muscle. *Biophys. J.* **63**, 387–396.
25. Kensler, R. W., Peterson, S. & Norberg, M. (1994). The effects of changes in temperature or ionic strength on isolated rabbit and fish skeletal muscle thick filaments. *J. Muscle Res. Cell Motil.* **15**, 69–79.
26. Geeves, M. A. & Holmes, K. C. (1999). Structural mechanism of muscle contraction. *Annu. Rev. Biochem.* **68**, 687–728.
27. Reubold, T. F., Eschenburg, S., Becker, A., Kull, F. J. & Manstein, D. J. (2003). A structural model for actin-induced nucleotide release in myosin. *Nature Struct. Biol.* **10**, 826–830.
28. Holmes, K. C., Angert, I., Kull, F. J., Jahn, W. & Schröder, R. R. (2003). Electron cryo-microscopy shows how strong binding of myosin to actin releases nucleotide. *Nature*, **425**, 423–427.
29. Zoghbi, M. E., Padrón, R. & Craig, R. (2003). Helical order in tarantula myosin filaments requires the closed conformation of the myosin head. *Biophys. J.* **84**, 562a.
30. Hidalgo, C., Padrón, R., Horowitz, R., Zhao, F. Q. & Craig, R. (2001). Purification of native myosin filaments from muscle. *Biophys. J.* **81**, 2817–2826.
31. Rayment, I., Rypniewski, W. R., Schmidt-Base, K., Smith, R., Tomchick, D. R., Benning, M. M. *et al.* (1993). Three-dimensional structure of myosin subfragment-1: a molecular motor. *Science*, **261**, 50–58.
32. Fisher, A. J., Smith, C. A., Thoden, J. B., Smith, R., Sutoh, K., Holden, H. M. & Rayment, I. (1995). X-ray structures of the myosin motor domain of *Dictyostelium discoideum* complexed with MgADP.BeFx and MgADP.AIF₄. *Biochemistry*, **34**, 8960–8972.
33. Gulick, A. M., Bauer, C. B., Thoden, J. B. & Rayment, I. (1997). X-ray structures of the MgADP, MgATP γ S, and MgAMPPNP complexes of the *Dictyostelium discoideum* myosin motor domain. *Biochemistry*, **36**, 11619–11628.
34. Houdusse, A., Szent-Györgyi, A. G. & Cohen, C. (2000). Three conformational states of scallop myosin S1. *Proc. Natl Acad. Sci. USA*, **97**, 11238–11243.
35. Bauer, C. B., Holden, H. M., Thoden, J. B., Smith, R. & Rayment, I. (2000). X-ray structures of the apo and MgATP-bound states of *Dictyostelium discoideum* myosin motor domain. *J. Biol. Chem.* **275**, 38494–38499.
36. Smith, C. A. & Rayment, I. (1996). X-ray structure of the magnesium(II).ADP.vanadate complex of the *Dictyostelium discoideum* myosin motor domain to 1.9 Å resolution. *Biochemistry*, **35**, 5404–5417.
37. Domínguez, R., Freyzon, Y., Trybus, K. M. & Cohen, C. (1998). Crystal structure of a vertebrate smooth muscle myosin motor domain and its complex with the essential light chain: visualization of the pre-power stroke state. *Cell*, **94**, 559–571.
38. Houdusse, A., Kalabokis, V. N., Himmel, D., Szent-Györgyi, A. G. & Cohen, C. (1999). Atomic structure of scallop myosin subfragment S1 complexed with MgADP: a novel conformation of the myosin head. *Cell*, **97**, 459–470.
39. Himmel, D. M., Gourinath, S., Reshetnikova, L., Shen,

- Y., Szent-Györgyi, A. G. & Cohen, C. (2002). Crystallographic findings on the internally uncoupled and near-rigor states of myosin: further insights into the mechanics of the motor. *Proc. Natl Acad. Sci. USA*, **99**, 12645–12650.
40. Malnasi-Csizmadia, A., Woolley, R. J. & Bagshaw, C. R. (2000). Resolution of conformational states of Dictyostelium myosin II motor domain using tryptophan (W501) mutants: implications for the open-closed transition identified by crystallography. *Biochemistry*, **39**, 16135–16146.
41. Malnasi-Csizmadia, A., Pearson, D. S., Kovacs, M., Woolley, R. J., Geeves, M. A. & Bagshaw, C. R. (2001). Kinetic resolution of a conformational transition and the ATP hydrolysis step using relaxation methods with a Dictyostelium myosin II mutant containing a single tryptophan residue. *Biochemistry*, **40**, 12727–12737.
42. Wray, J. & Jahn, W. (2002). γ -Amido-ATP stabilizes a high-fluorescence state of myosin subfragment 1. *FEBS Letters*, **518**, 97–100.
43. Xu, S., Offer, G., Gu, J., White, H. D. & Yu, L. C. (2003). Temperature and ligand dependence of conformation and helical order in myosin filaments. *Biochemistry*, **42**, 390–401.
44. Takemori, S., Yamaguchi, M. & Yagi, N. (1995). An X-ray diffraction study on a single frog skinned muscle fiber in the presence of vanadate. *J. Biochem. (Tokyo)*, **117**, 603–608.
45. Craig, R., Padrón, R. & Kendrick-Jones, J. (1987). Structural changes accompanying phosphorylation of tarantula muscle myosin filaments. *J. Cell Biol.* **105**, 1319–1327.
46. Stewart, M. (1988). Computer image processing of electron micrographs of biological structures with helical symmetry. *J. Electron Microsc. Tech.* **9**, 325–358.
47. Panté, N., Sosa, H. & Padrón, R. (1986). Prediction of relative changes in the equatorial X-ray diffraction pattern of striated muscle caused by the activation of muscle contraction. *Acta Cient. Venez.* **37**, 223–225.
48. Sosa, H., Panté, N. & Padrón, R. (1988). Analysis of the equatorial section of X-ray diffraction patterns of striated muscles of tarantulas under various experimental conditions. *Acta Cient. Venez.* **39**, 51–59.
49. Egelman, E. H. & Padrón, R. (1984). X-ray diffraction evidence that actin is a 100 Å filament. *Nature*, **307**, 56–58.
50. Irving, T. C. & Maughan, D. W. (2000). *In vivo* X-ray diffraction of indirect flight muscle from *Drosophila melanogaster*. *Biophys. J.* **78**, 2511–2515.
51. Miller, A. & Tregear, R. T. (1972). Structure of insect fibrillar flight muscle in the presence and absence of ATP. *J. Mol. Biol.* **70**, 85–104.
52. Wray, J. (1982). Organization of myosin in invertebrate thick filaments. In *Basic Biology of Muscles: A Comparative Approach* (Twarog, B. M., Levine, R. J. & Dewey, M. M., eds), pp. 29–36, Raven Press, New York.
53. Millman, B. M. & Bennett, P. M. (1976). Structure of the cross-striated adductor muscle of the scallop. *J. Mol. Biol.* **103**, 439–467.
54. Zhao, F. Q. & Craig, R. (2003). Ca^{2+} causes release of myosin heads from the thick filament surface on the milliseconds time scale. *J. Mol. Biol.* **327**, 145–158.
55. Ménétret, J. F., Hofmann, W. & Lepault, J. (1988). Cryo-electron microscopy of insect flight muscle thick filaments. An approach to dynamic electron microscope studies. *J. Mol. Biol.* **202**, 175–178.
56. Goodno, C. C. (1979). Inhibition of myosin ATPase by vanadate ion. *Proc. Natl Acad. Sci. USA*, **76**, 2620–2624.
57. Marston, S. B., Rodger, C. D. & Tregear, R. T. (1976). Changes in muscle crossbridges when β , γ -imido-ATP binds to myosin. *J. Mol. Biol.* **104**, 263–276.
58. Abbott, R. H. & Leech, A. R. (1973). Persistence of adenylate kinase and other enzymes in glycerol extracted muscle. *Pflugers Arch.* **344**, 233–243.
59. Goody, R. S., Holmes, K. C., Mannherz, H. G., Leigh, J. B. & Rosenbaum, G. (1975). Cross-bridge conformation as revealed by X-ray diffraction studies on insect flight muscles with ATP analogues. *Biophys. J.* **15**, 687–705.
60. Yount, R. G., Babcock, D., Ballantyne, W. & Ojala, D. (1971). Adenylyl imidodiphosphate, an adenosine triphosphate analog containing a P–N–P linkage. *Biochemistry*, **10**, 2484–2489.
61. Maruta, S., Henry, G. D., Sykes, B. D. & Ikebe, M. (1993). Formation of the stable myosin-ADP-aluminum fluoride and myosin-ADP-beryllium fluoride complexes and their analysis using ^{19}F NMR. *J. Biol. Chem.* **268**, 7093–7100.
62. Chabre, M. (1990). Aluminofluoride and beryllifluoride complexes: a new phosphate analogs in enzymology. *Trends Biochem. Sci.* **15**, 6–10.
63. Henry, G. D., Maruta, S., Ikebe, M. & Sykes, B. D. (1993). Observation of multiple myosin subfragment 1-ADP-fluoroberyllate complexes by ^{19}F NMR spectroscopy. *Biochemistry*, **32**, 10451–10456.
64. Zoghbi, M. E. (2003) *Importancia de la conformación de la cabeza de miosina para el orden helical en los filamentos gruesos de músculo estriado de invertebrados estudiados mediante microscopía electrónica*. PhD thesis, Centro de Estudios Avanzados, Instituto Venezolano de Investigaciones Científicas.

Edited by W. Baumeister

(Received 4 March 2004; received in revised form 25 June 2004; accepted 6 July 2004)